GUASNR

SSM-Wheat: a simulation model for wheat development, growth and yield

A. Soltani[a,*], V. Maddah[a], T.R. Sinclair[b]

[a]Agronomy Group, Gorgan University of Agricultural Sciences and Natural Resources, Gorgan 49138-15739, Iran.
[b]Department of Crop Science, North Carolina State University, Raleigh, NC 27695-7620, USA.
*Corresponding author. E-mail: afsoltani@yahoo.com

Abstract

A robust crop model can assist in genetic improvement and cultural management of the crop. The objectives of this study were to describe a wheat (*Triticum aestivum* L.) model and to report results of its evaluation. The model simulates phenological development, leaf development and senescence, crop mass production and partitioning, plant nitrogen balance, yield formation and soil water and nitrogen balances. The model includes responses of crop processes to environmental factors of solar radiation, temperature and nitrogen and water availability. Parameters are inputted in describing physiological processes so that these can be varied to define genotypic differences. The model uses a daily time step and readily available weather and soil information. The model was tested using independent data and indicated an acceptable performance for important crop attributes as compared to observed results including days to anthesis (CV=4.5%; r=0.98) and maturity (CV=5.6%; r=0.96), crop LAI (CV=11.8%; r=0.80) and dry mass at anthesis (CV=9.3%; r=0.72) and total crop mass (CV=9.5%; r=0.82) at maturity and grain yield (CV=8.4%; r=0.89). It was concluded that the model can be used in simulation studies of wheat yield and its limitations in response to environmental conditions, management inputs and genetic factors.

Keywords: Wheat; Simulation; Yield; Water; Nitrogen.

Introduction

Crop simulation models are mathematical representations of plant growth processes as influenced by interactions among genotype, environment and

crop management. Using crop simulation models can be an efficient complement to experimental research (Soltani and Sinclair, 2012a). Models are being used to understand the response of crops to possible changes in crop traits (Sinclair et al., 2010; Soltani and Sinclair, 2012b; Soltani and Sinclair, 2012c), cultural management (Soltani et al., 2001a; Soltani and Hoogenboom, 2007) and environmental variables (Soltani et al., 2001b).

Soltani and Sinclair (2012a) presented principles and procedures in developing simple, mechanistic crop models. In their textbook, they developed and presented quantitative hypotheses for the key processes in crop development, growth and yield. The emphasis was on functions that required the fewest assumptions and were appropriate over a range of conditions. They included a step-by-step development of a wheat (*Triticum aestivum* L.) crop model as a practical example. The wheat model included all important physiological aspects of wheat crop under radiation-, water-, and nitrogen-limited conditions. This wheat model is in fact an up-to-date version of earlier wheat models developed by Sinclair and co-workers (Amir and Sinclair, 1991; Sinclair and Amir, 1992; Soltani and Sinclair, 2012a). Soltani and Sinclair (2012a), however, did not indicate how robust their model was.

While there are many simulation models for wheat and some of them are very well-known, the reasons for development of the current model are (Soltani and Sinclair, 2012a):

(1) Many models are not adequately transparent. Transparency means that model parameters, flow diagrams and code can be readily understood by those that were not involved in its development.

(2) Many models use extensive reductionism which means the model includes many equations and parameters for each crop key process. In some cases, models are so complex that aspects of their structure and performance are not clear even to members of the modeling team (Monteith, 1996). Adding complexity within a model does not necessarily move the model closer to reality. In fact, it is quite likely that including hypotheses without extensive experimental justification can easily increase the imperfection of the model (Sinclair and Seligman, 1996). Users have to use these models as 'black-boxes' without a clear understanding of the model structures and limitations. Complex models need considerable input data that may not be easily available.

(3) In the case of many well-known crop models, codes are not accessible, or if they are, they are not the same as model documents.

(4) Sometimes the model software is not clear, simple, intuitive and flexible. In such cases, users have to struggle with the interface rather than focus on how the model works.

(5) Many models include one or more parameters with opaque meaning. We believe all crop and cultivar parameters should have a clear meaning and should be directly measure able.

This paper presents a brief description of the wheat model of Soltani and Sinclair (2012a) and a complete description of modifications that were necessary to obtain a wheat model for research purposes. The model is designed to assist crop improvement and management research under various conditions of crop growth and yield. The paper also reports the results of a model robustness test.

Materials and Methods

Model structure

Detailed description of the model structure, procedures needed for model parameterization and model troubleshooting can be found in Soltani and Sinclair (2012a). In this section we only provide a brief, overview description of the model structure and modifications of the original model.

Phenology

Stages of development of emergence, first-tiller, first-node, ligule of flag leaf visible, ear emergence, anthesis, physiological maturity and harvest maturity are predicted by the model. The original model only included emergence, ligule of flag leaf visible (termination leaf production on main stem), beginning seed growth (few days after anthesis), termination seed growth (physiological maturity) and harvest maturity. Calculation of phenological development in the model is based on the biological day concept (Soltani and Sinclair, 2012a). A biological day is a day with optimal temperature, photoperiod and moisture conditions for plant development. Each day from sowing until maturity, biological day (*BD*) is obtained by multiplying temperature (*tempfun*), photoperiod (*ppfun*), vernalization (*verfun*) and water-deficit (*wsfd*) functions (factors):

$DB_t = tempfun \times ppfun \times verfun \times wsfd$ (1)

Cumulative biological day is then obtained from integration of daily biological days. A phenological stage is predicted to occur if cumulative biological days is just reached or exceeds the biological days required for achieving that stage. Biological day requirement of different phenological stages are inputs of the model (Appendix I).

Daily mean temperature is used to find the temperature function (0-1) that accounts for the effect of temperature on development rate. The photoperiod function (0-1) that accounts for the effect of photoperiod on development rate if the stage is sensitive to photoperiod is obtained from daily photoperiod. Soltani and Maddah (2013) analyzed phenological data from a wide range of sowing dates and different years (Table 1) using the approach presented by Soltani et al. (2006a) and Soltani and Sinclair (2012a). They indicated that a beta function for temperature and a quadratic function for photoperiod gave best results. Schematics of the functions are presented in Figure 1a and 1b, respectively. The original model used a 3-segment function for temperature function and a 2-segment for photoperiod function.

Table 1. Experiments used for parameterization and evaluation of SSM-Wheat model.

Experiment location and season	treatments	reference
Experiments used for parameter estimation		
Gorgan, 2005-2006	Genotype, planting date	Arab-ameri, 2008
Gorgan, 2005-2006	Genotype, planting date	Ahmadi, 2008
Gorgan, 2005-2006	Genotype, vernalization period	Mirdavardoost, 2008
Gorgan, 2005-2006	Genotype, planting date	Khavari, 2008
Gorgan, 2008-2009	Genotype, water regime	Bakhshandeh, 2011
Gorgan, 2008-2009	Genotype, water regime	Ghadiryan, 2011
Gorgan, 2012-2013	Genotype, plant density	Zafari, 2013
Experiments used for model evaluation		
Gorgan, 2005-2006	Genotype	Maddah, 2007
Gorgan, 2006-2007	Genotype, plant density	Jafari, 2008
Gorgan, 2006-2007	Genotype, 17 farmers' fields	Zeinali, 2009
Gorgan, 2007-2008	Genotype, planting date	Dastmalchi, 2010
Gorgan, 2007-2008	Genotype, nitrogen fertilizer rate	Hosseini, 2010
Gorgan, 2007-2008	Genotype, plant density	Zahed, 2010

The beta function (Yan and Hunt, 1999) used to describe the temperature response is:

$$tempfun = [(T_c - T) / (T_c - T_o)] \times [(T - T_b) / (T_o - T_b)]^{[(T_o - T_b)/(T_c - T_o)]} \qquad (2)$$
$$\text{if} \quad T_b < T < T_c$$
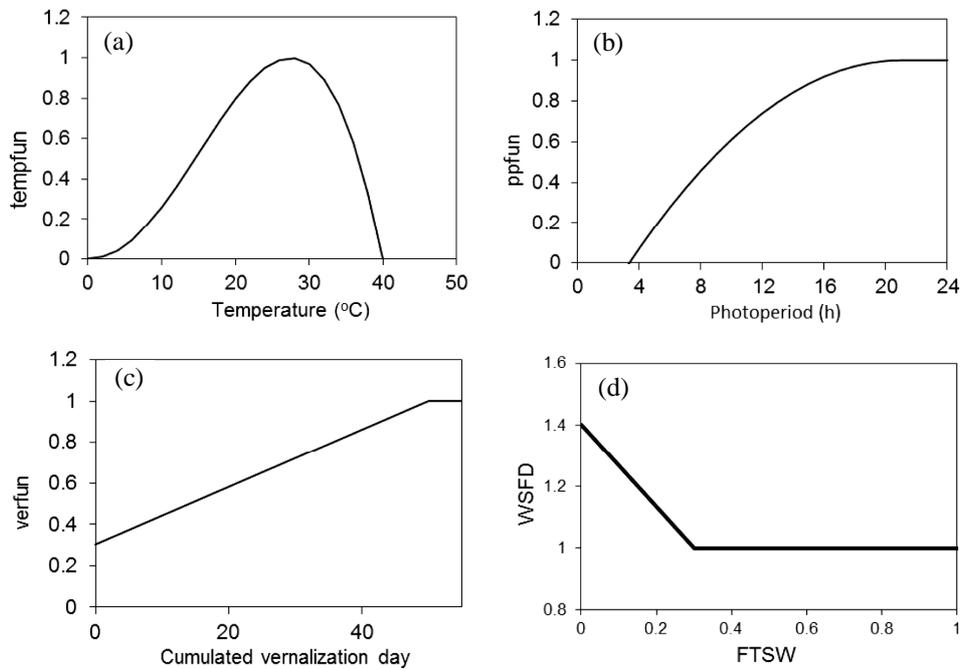$$tempfun = 0 \qquad \qquad \text{if} \quad T \le T_b \ or \ T \ge T_c$$

Figure 1. Schematic representation of beta function to calculate temperature factor (a; *tempfun*), quadratic function to calculate photoperiod function (b; *ppfun*) and a two-pieces function to calculate vernalization (c; *verfun*) and water deficit functions (d; WSFD).

where T is temperature, T_b the base temperature, T_o the optimum temperature and T_c the ceiling temperature. Soltani and Maddah (2013) found 0 °C for T_b, 21 °C for T_o and 40 °C for $T_c$across several wheat cultivars are (Appendix I).

The quadratic function (Soltani et al., 2006a) used to describe the long-day photoperiod response of wheat is:

$$ppfun = 1 \qquad\qquad if \qquad PP \geq P_c \qquad\qquad (3)$$
$$ppfun = 1-ppsen\ (CPP-PP)^2 \qquad if \qquad PP < P_c$$

where PP is photoperiod (h d^{-1}), CPP the critical photoperiod below which development rate decreases due to short photoperiod and *ppsen* the photoperiod sensitivity coefficient. In the model CPP is constant (21 h) for different cultivars, but *ppsen* ranges between 0.00785 to 0.0090 among cultivars according to Soltani and Maddah (2013; Appendix I).

The vernalization factor (0-1) is obtained from cumulative vernalization days experienced by the crop up to the current day, total amount of vernalization days needed to saturate the vernalization response (VDSAT), and a sensitivity coefficient (*vsen*) (Ritchie, 1991; Soltani and Sinclair, 2012a; Figure 1):

$$\text{\textit{verfun} = 1–\textit{vsen}} \; (\text{VDSAT–CUMVER}_i) \quad \textit{if} \quad \text{CUMVER}_i < \text{VDSAT} \qquad (4)$$
$$\textit{verfun} = 1 \qquad\qquad\qquad\qquad \textit{if} \quad \text{CUMVER}_i \geq \text{VDSAT}$$

In the model a constant value of 50 days is assumed for VDSAT for all cultivars (Ritchie, 1991; Soltani and Maddah, 2013; Appendix I). From sowing to first-node, CUMVER is calculated by calculating and adding vernalization day experienced by the crop each calendar day (VERDAY) to the previous day CUMVER$_{i-1}$:

$$\text{CUMVER}_i = \text{CUMVER}_{i-1} + \text{VERDAY} \qquad\qquad\qquad (5)$$

VERDAY is 1.0 on a day when the plant is exposed to the optimum temperature for vernalization. The optimum temperature for vernalization in wheat is between 0 and 8 ^{o}C (Ritchie, 1991). Temperatures lower that -1°C or higher than 12 ^{o}C do not contribute to vernalization and the value of VERDAY is 0. For temperatures in the range of 0 to -1 ^{o}C and from 8 to 12 ^{o}C, the effectiveness in vernalization is decreased linearly and the value VERDAY is between 0 and 1.

High temperatures can cause de-vernalization during the early stages of vernalization (Ritchie, 1991). If a crop had already experienced 10 days of vernalization (CUMVER$_i$>10), occurrence of high temperatures will not result in de-vernalization. However, if cumulative vernalization day is lower than 10 days and maximum temperature (TMAX, ^{o}C) is higher than 30 ^{o}C, then cumulative vernalization day is reduced by 0.5 day per each degree greater than 30 ^{o}C.

It has been reported that wheat is responsive to photoperiod and vernalization from emergence to terminal spikelet (Ritchie, 1991). Here, this period is assumed to be from emergence to first-node or jointing (about 80 ^{o}C after terminal spikelet). The value of photoperiod and vernalization functions is set to 1 for stages that are not sensitive to photoperiod and vernalization.

Water deficit stress factor (1-1.4) is a scaling factor that accounts for the acceleration of development rate under drought (see below) (Soltani and Sinclair, 2011; Soltani and Sinclair, 2012a).

Leaf area development and senescence

To simulate leaf area expansion, the first step is to determine on each day the increase in leaf number on the main stem using the phyllochron (temperature unit between emergence of successive leaves) concept. Phyllochron values between 90 and 112 ^{o}C were found for cultivars of this study (Soltani and Maddah, 2013; Appendix I). Plant leaf area is then computed as a function of main stem leaf number and water and nitrogen availability (Soltani et al., 2006b; Soltani and Sinclair, 2011; Soltani and Sinclair, 2012a). Leaf production on main stem terminates at the appearance of the ligule of the flag leaf. Therefore, photoperiod, temperature, vernalization and water availability determine the time available for leaf production.

From emergence to flag leaf ligule appearance, potential plant leaf area each day (*y*) is predicted from main stem leaf number on that day (*x*) using a simple, power function (Soltani and Sinclair, 2012a; Figure 2a):

$$y = x^b \tag{6}$$

The coefficient of the function (*b*) is adjusted for plant density (Figure 2b). Increase in LAI is then computed from increase in plant leaf area between today and yesterday and plant density. This increase is further limited to the amount calculated based on nitrogen availability, which is nitrogen allocated to leaf growth (g N m^{-2} d^{-1}) divided by specific leaf nitrogen (g N m^{-2} leaf) (also see below).

From flag leaf ligule appearance until the beginning seed growth, leaf area development (due to leaf expansion on tillers) is calculated from dry matter allocated to leaf growth (10% of daily produced dry matter, see below) and specific leaf area. It is assumed that plant leaf area development stops at the beginning of seed growth.

Under N-limited conditions, the amount of leaf area senesced each day (DLAI, m^{2}m^{-2} d^{-1}) is computed from the amount of nitrogen mobilized from the leaves (XLN, g N m^{-2} ground) divided by the difference between specific leaf nitrogen of green (SPLNG, g N m^{-2} leaf) and senesced (SLNS, g N m^{-2} leaf) leaves (Sinclair et al., 2003):

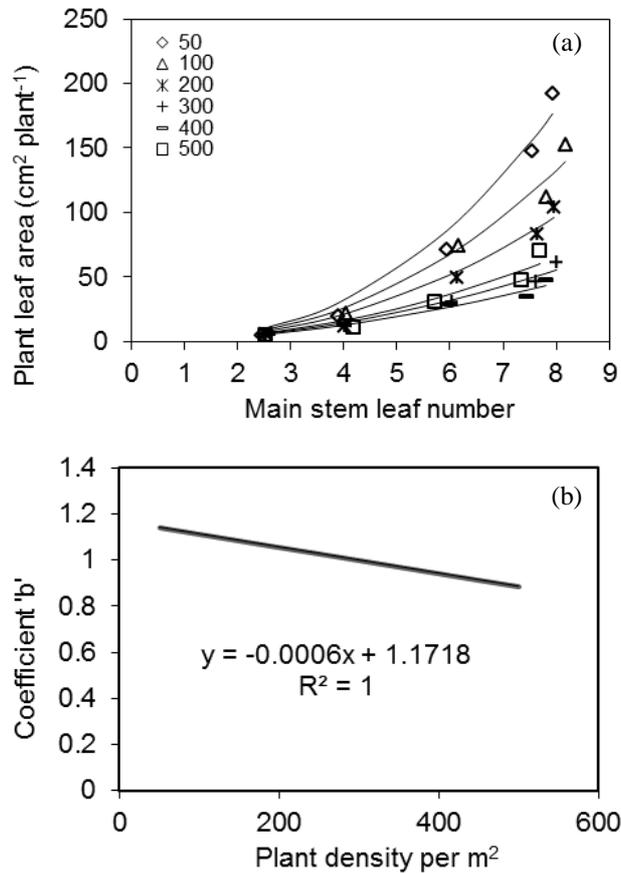$$DLAI = XLN / (SLNG - SLNS) \tag{7}$$

Figure 2. Plant leaf area as a function of main stem leaf number described by a power function as $y=x^b$ under different plant densities (a); numbers are plant densities. Dependency of the standardized coefficient of the power function on plant density (b). Data are from Zafari (2013).

However, under non-limiting N conditions where the model does not simulate plant and soil N balances, leaf senescence is simulated by decreasing LAI linearly to 0 from the beginning seed growth to harvest maturity.

Minimum temperatures lower than -5 $^{\circ}$C (freezing events) can result in LAI destruction which was not included in the original model. Here, it is assumed 1% of crop LAI is lost for each degree of minimum temperature below -5 $^{\circ}$C. Thus, an event of minimum temperature of -15 $^{\circ}$C will destroy 10% of the current crop LAI (Williams et al., 1989).

Crop mass production and partitioning

Daily increase of crop mass is estimated as the product of incident photosynthetic active radiation (PAR, MJ m^{-2} d^{-1}), the fraction of that radiation intercepted by the crop (FINT) and efficiency with which the intercepted PAR is used to produce crop dry mass, i.e., radiation use efficiency (RUE, g MJ^{-1}) (Soltani and Sinclair, 2011; Soltani and Sinclair, 2012a). The fraction of intercepted radiation is determined from crop leaf area index (LAI) and crop canopy extinction coefficient (*KPAR*):

$$FINT = 1 - \exp(-KPAR \times LAI) \tag{8}$$

The daily value of RUE is obtained as (Soltani and Sinclair, 2012a):

$$RUE = IRUE \times TCFRUE \times WSFG \times CO2RUE \tag{9}$$

where IRUE is potential RUE and TCFRUE, WSFG and CO_2 RUE are scalar factors (0-1) that adjust IRUE for temperature, water deficit and atmospheric CO_2 concentration, respectively. Correction for CO_2 concentration is based on Ludwig and Asseng (2006).

Daily dry mass production is partitioned between three sinks: leaves, grains and other organs (stems, leaf sheaths and ears excluding grains; we call this sink 'stem' hereafter) (Soltani and Sinclair, 2011; Soltani and Sinclair, 2012a). Critical phenological stages for dry matter partitioning are: flag leaf ligule appearance (when leaf production on the main stem terminates, TLM), beginning seed growth (BSG) or beginning linear increase in harvest index and termination of seed growth (TSG) or cessation of linear increase in harvest index. BSG occurs 5 biological days after anthesis and TSG occurs 1.5 biological days before physiological maturity (Soltani and Maddah, 2013). Leaf and 'stem' are active growing organs from emergence until TLM.

A biphasic pattern is used for crop mass partitioning between leaf and stem before TLM (Soltani et al., 2006c; Soltani and Sinclair, 2011). At lower levels of total dry matter, a higher portion of dry matter is allocated to leaves (phase 1), but at higher levels of total dry matter (i.e., under favorable conditions for vegetative growth) more dry matter goes to stems (phase 2) (Figure 3). Based on the analysis of Soltani and Maddah (2013; Appendix I), mean values for leaf and stem partitioning coefficients were 0.6 and 0.4, respectively, during phase 1 when crop mass had not achieved 160 g m^{-2}.

Above crop mass of 160 g m^{-2}, phase 2 occurs and the leaf and stem partitioning coefficients were 0.3 and 0.7, respectively. In the period from TLM to BSG, 10% of daily increase in dry matter is partitioned to the leaves and the remaining goes to the 'stem'. After BSG, all the daily dry matter production goes to the grain. However, if there is surplus of dry matter in excessive of the grain requirements (see below), the excess dry matter goes to the 'stems'.
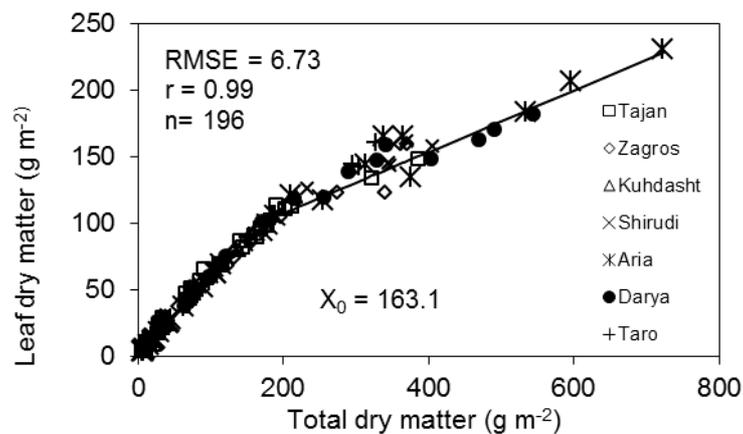

Figure 3. Relationship between cumulative leaf dry matter versus total dry matter from emergence to ligule of flag leaf visible for several wheat cultivars. Data are from Bakhshandeh (2011) and Ghadiryan (2011).

Plant nitrogen balance

Plant N balance is simulated differently in the stages before and after seed growth (Sinclair et al., 2003; Soltani and Sinclair, 2011; Soltani and Sinclair, 2012a). Before seed growth, daily demand for N accumulation (PNUP, g N m^{-2} d^{-1}) is computed from daily increase in LAI (GLAI), specific leaf N in green leaves (SLNG, g N m^{-2} leaf), daily increase in 'stem' dry matter (GST g m^{-2} d^{-1}) and N concentration in green stems (SNCG, g g^{-1}).

$$PNUP = GLAI \times SLNG + GST \times SNCG \qquad (10)$$

A constant value of SLNG of 1.5 g N m^{-2} leaf is used in the model (Soltani and Sinclair, 2012a). SNCG of 15 mg g^{-1} is used and assumed to be the target stem N concentration when N is not limited. Daily demand for N

accumulation is then adjusted to obtain daily N uptake (NUP). However, limitation on N accumulation are considered. (1) Maximum rate of N accumulation in wheat is 0.25 g m^{-2} d^{-1} (Sinclair and Amir, 1992; Soltani and Sinclair, 2012a). Therefore, under conditions that demand is higher than this value, actual rate of N accumulation is limited to this value. (2) N accumulation is sensitive to flooding conditions. NUP is set to zero under soil saturation conditions. (3) NUP is limited to the amount of soil N available for crop uptake (SNAVL, see below). Thus, if NUP is calculated to be greater than SNAVL, it is adjusted to the value of SNAVL.

At times when N accumulation rate does not fully meet the demand, the following responses occur sequentially (Soltani and Sinclair, 2011; Soltani and Sinclair, 2012a). First, the concentration of stem N is allowed to decrease. The decrease is continued until stem N concentration reaches its minimum, 5 mg g^{-1} (Sinclair and Amir, 1992; Soltani and Maddah, 2013). Under more severe N deficit when stem N concentration reaches its minimum, the next response is modeled as an inhibition in leaf area development and continued stem growth at minimum N concentration. Under extreme N limitation where setting new leaf area development to zero still does not provide sufficient N for stem growth, leaves are senesced as sources of remobilized N. This means that leaf senescence is possible during vegetative growth under limited N accumulation. The N content of the senesced leaves is 0.4 g N m^{-2} (Sinclair and Amir, 1992; Soltani and Maddah, 2013). Therefore, remobilizable N content from leaves is 1.1 g m^{-2} (difference between 1.5 and 0.4 g m^{-2}).

After BSG, seeds become the prime sink for N and daily N demand by the seeds is calculated as the product of seed growth rate (see below) and seed N concentration. Seed N concentration is held constant at 21 mg g^{-1} in the model (Soltani and Maddah, 2013). NUP is then set equal to daily N demand by seeds as it is assumed that grains are the only sink during seed growth (see below). All the limitation described above for limiting N uptake during the vegetative stage, apply in seed growth. In addition, NUP is set equal to zero when daily dry matter production by the crop does not exceed SGR, which means there is no excess photosynthate to support NUP. When N uptake from the soil does not take place or is not adequate to meet the full requirements of the growing seeds, N is translocated from the leaves and stems to the seeds. The fraction of the N translocated from leaves and stems is based on the relative amount of translocatable N in each tissue. That is:

$$TRLN = LAI \times (SLNG - SLNS) + (NST - WST \times SNCS) \tag{11}$$

$$FXLF = LAI \times (SLNG - SLNS) / TRLN \tag{12}$$

where TRLN is the translocatable N from leaves and 'stem', NST the N content of 'stem', WST the 'stem' dry weight and FXLF the fraction of translocatable N from the leaves. Using FXLF, daily decrease in leaf N (XNLF, g N m^{-2} d^{-1}) and stem N (XNST, g N m^{-2} d^{-1}) are computed:

$$XLFN = (SGR \times GNC - NUP) \times FXLF \tag{13}$$

$$XNST = (SGR \times GNC - NUP) \times (1 - FXLF) \tag{14}$$

N mobilization from leaves results in leaf senescence and reduction in PAR interception and consequently mass production. RUE is assumed independent from leaf N content and N remobilization results in leaf senescence and not decrease in leaf [N] (Soltani and Sinclair, 2011; Soltani and Sinclair, 2012a).

Yield formation

Yield formation in the original model is simply simulated as total dry matter production during seed filling period plus a fraction of crop dry mass at BSG (as mobilized dry matter). Modeling seed growth rate and yield formation in the current model is based on a modified linear increase in harvest index concept as described by Soltani and Sinclair (2011). Seed growth rate (SGR, g m^{-2} d^{-1}) is simulated based on linear increase in harvest index, but actual daily seed growth rate is limited to current crop photosynthesis plus daily rate of mobilized dry matter from vegetative organs. The slope of the linear increase in harvest index (dHI/dt) is adjusted for pre-seed growth conditions experienced by the crop.

Arabameri et al. (2010) and Fletcher and Jamieson (2006) indicated that dHI/dt varied and this variation was related to total crop mass at the beginning of seed growth. Based on combination of the data from these two studies (Figure 4), in the current model a scaling factor (between 0 and 1) is calculated from crop mass at BSG; when total mass at beginning seed growth is between 600 and 1200 g m^{-2}, the scaling factor is at its maximum (=1), but it decreases linearly at lower and higher levels of mass at BSG and reaches zero at 0 and 3200 g m^{-2}, respectively. In the model, dHI/dt is calculated at BSG as a product of the scaling factor and potential dHI/dt (PDHI) of the cultivar being simulation. Then, daily SGR is calculated using

the dHI/dt. The actual SGR calculated each day is further limited to daily crop mass production and the mobilization of dry matter accumulated in vegetative organs before seed growth period. The mobilization occurs only if daily dry matter production is lower than SGR calculated from dHI/dt. Fraction of mobilizeable dry matter is considered to be 22% at total crop mass at BSG (Soltani and Maddah, 2013). In addition, SGR is set to zero if there is no N for seed growth from the soil or N retranslocation from leaves and stems.
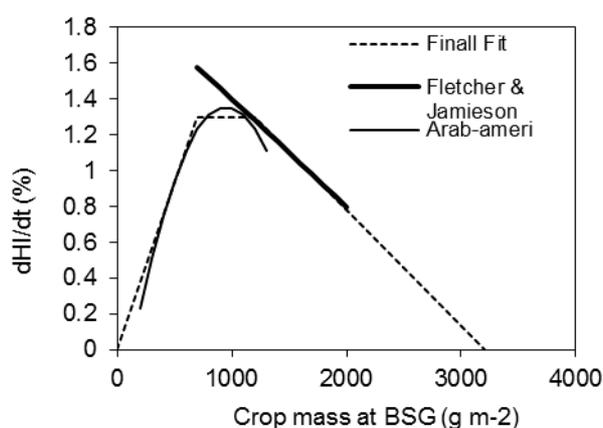

Figure 4. Dependency of linear increase in harvest index (dHI/dt, %) to total crop mass at beginning seed growth (BSG) based on Fletcher and Jamieson (2006) for New Zealand cultivars and conditions and Arabameri et al. (2010) for Gorgan cultivars and conditions, and a line fitted by eye to describe the overall dependency.

Soil water balance

The model can simulate soil water balance and the effects of soil water deficit on plant development and growth. The original model used a 2-layer soil for calculation of soil water balance; a top layer and a root zone layer. In the current model, up to 10 soil layers can be used in the calculation of soil water balance. In both models, soil water balance calculations are mainly based on the approach of Amir and Sinclair (1991), van Laar et al. (1997) and Ritchie (1998). The input soil parameters are volumetric soil water content (m^3 m^{-3}) at saturation (SAT) and drained upper limit (DUL), extractable soil water content (EXTR), drainage factor (DRAINF) and soil moisture availability index for each layer (Table 1). Soil water content at the

lower limit is calculated as DUL minus EXTR. The water content when the soil is air-dried is computed as the lower limit divided by 3. Soil moisture availability index has a value of 0 at the lower limit and 1 at the drained upper limit. Soil albedo (for calculation of evapotranspiration) and soil curve number (for calculation of run-off) are also needed.

Soil water content of each layer (WL, mm) in each day (i) is obtained as:

$$WL(L)_i = WL(L)_{i-1} + FLIN(L) - WU(L) - SE(L) - FLOUT(L) \tag{15}$$

where L is the layer number, FLIN the water flux into the layer, WU the amount of transpiration water extracted from the layer, SE the amount of soil evaporation water extracted from the layer and FLOUT is the downward water flux that leaves a layer. For the top layer, FLIN is calculated as rainfall plus irrigation minus surface run-off. For the remaining deeper layers, downward water flux is taken as FLOUT of the upper layer.

Actual transpirable soil water (ATSW, mm), total transpirable soil water (TTSW, mm) and fraction transpirable soil water (FTSW, mm mm^{-1}) are obtained as:

$$ATSW(L) = WL(L) - WLLL(L) \tag{16}$$

$$TTSW(L) = WLUL(L) - WLLL(L) \tag{17}$$

$$FTSW(L) = ATSW(L) / TTSW(L) \tag{18}$$

where WLLL is the layer water content at lower limit and WLUL is the layer water content at drained upper limit, both expressed in mm.

Drainage from each layer (FLOUT) is obtained using the approach of Ritchie (1998). FLOUT from the user-specified layer (usually the deepest layer) is considered as deep drainage. Only a fraction of soil water content above the upper limit is allowed to leave a layer each day. The fraction is called drainage factor (DRAINF).

Run-off is calculated using a modified curve number technique (Williams, 1991; Jones et al., 2003) as described by Soltani and Sinclair (2012a). It is a function of soil curve number, soil water content at lower limit and saturation, actual soil water content in the two first layers and daily rainfall. Curve numbers are assigned to various soils depending on their texture. It was assumed that run-off does not take place under irrigated conditions, so all irrigation or rainfall water infiltrate into the soil.

Soil evaporation is calculated using a two-stage soil evaporation model (Amir and Sinclair, 1991; Soltani and Sinclair, 2012a). Stage I evaporation occurs when water is present in the top layer and FTSW of the total root zone is greater than 0.5. Potential evaporation rate is calculated according to a modified Priestly and Taylor model (Priestly and Taylor, 1972; Ritchie, 1998). Stage II evaporation occurs when the water in the top layer is exhausted or total root zone FTSW is less than 0.5. In Stage II, the potential rate of soil evaporation is also calculated as Stage I, but it is decreased substantially as a function of the square root of time since the start of Stage II. The calculation of soil evaporation returns to Stage I only when rain or irrigation of greater than 10 mm occurs. Evaporation water is extracted from the layers (SE(L)) with a preference from the top layer, then the second layer and so on. Only a fraction of soil water between actual soil water of a layer and its water content when it is air-dried is available for extraction each day. Thus, evaporation water extraction is possible from all layers so that redistribution of water due to developing potential gradients is mimicked (van Laar et al., 1997).

Daily transpiration rate is calculated directly from the daily rate of crop mass production, using a transpiration efficiency coefficient and vapor pressure deficit (Tanner and Sinclair, 1983; Soltani and Sinclair, 2012a). The transpiration efficiency coefficient is 5.8 Pa for wheat (Amir and Sinclair, 1991; Sinclair, 1994). The calculation of daily VPD was suggested by Tanner and Sinclair (1983) to be approximately 0.75 of the difference between saturated vapor pressure calculated from daily maximum and minimum temperatures. It was assumed that transpiration occurs from each layer with root (WU(L)) as a function of water content of the layer. This loss decreases to zero in a layer as its FTSW approaches zero. Consequently, as a layer dries less of the crop transpirational water is derived from that layer.

The model accounts for water additions from precipitation, irrigation and increasing soil layer thickness due to root growth. Daily rainfall is obtained from weather data and includes snow melt (cf. Soltani and Sinclair, 2012a) if necessary. The model can be used to explore the consequences of various irrigation schemes such as automatic irrigation or irrigation at specific crop growth stages or dates.

As roots penetrate into a layer, there is an increase in the amount of water available to the crop if the layer contains water. The initial root depth is 200

mm at emergence and potential rate of root penetration (GRTDP) into the soil is considered 30 mm per biological day. The actual penetration rate is obtained as the product of the potential rate and biological day per calendar day (BD). The extension rate is set to zero before emergence and after beginning seed growth. Similarly, the root extension rate is set to zero if daily dry matter production is zero or the soil layer is dry (ATSW=0), or the root depth has already reached its maximum depth or soil depth. The root depth calculated by the model is effective rooting depth (root length density ≥ 0.1 cm cm^{-3}, van Laar et al., 1997; Dardanelli et al., 2004) and is different from maximum rooting depth.

The effect of water deficit is incorporated by calculating three scalar drought stress factors: growth (WSFG), leaf development (WSFL) and phenological development (WSFD). The value of WSFG and WSFL is equal to 1 while root zone FTSW is higher than specific thresholds related to each of them. By decreasing FTSW, below the thresholds, the value of the factors decline and are zero at FTSW=0. The thresholds are 0.3 for growth (WSSG=0.3) and 0.4 for leaf development (WSSL=0.4) (Amir and Sinclair, 1991; Soltani and Sinclair, 2012a). WSFG and WSFL are used as multipliers to RUE and daily increase in LAI, respectively.

Water deficit can hasten phenological development in wheat (Mc Master et al., 2009). This effect is simulated by calculating a scaling factor (WSFD). When water is not limited for mass production (FTSW>WSSG), development is not influenced by water deficit (WSFD=1). However, with development of water deficit for growth, phenological development is hastened. Maximum increase in development rate is considered to be 40% (WSSD=0.4) corresponding to WSFD=1.4. Acceleration in development rate is modeled by multiplying biological day calculated in each day after emergence by WSFD.

Flooding can also impede different physiological processes in wheat. On any day when soil water in the root layer is 95% or greater of soil water at saturation, all water stress factors (WSFL, WSFG and WSFD) are set to 0 (Soltani and Sinclair, 2012a). Further, it is considered that a certain number of consecutive flooding days (FLDKL) can result in crop death. FLDKL is assumed 20 d, but this can be changed if necessary.

Soil nitrogen balance

The original model simulates soil N balance only in the soil top layer. However, the current model simulates soil N balance in up to 10 layers as specified by user. Simulation of soil N is based on a simple soil N submodel successfully used by Sinclair and Amir (1992), Sinclair and Muchow (1995) and Sinclair et al. (1997) in their wheat, maize and sorghum models. For a complete description of the details refer to Soltani and Sinclair (2012a). Soluble N in the soil solution (NSOL, g N m^{-2}) is computed as:

$$NSOL(L)_i = NSOL(L)_{i-1} + NMIN(L) + NFERT(L) - NVOL(L) \qquad (19)$$
$$- NOUT(L) - NDNIT(L) - NUP(L)$$

where NMIN is the net mineralization rate (mineralization- immobilization) of organic matter, NFERT the N from fertilizer application, NVOL the N volatilization rate, NOUT the amount of N that leaves a layer (N leached from the layer), NDNIT the N denitrification rate and NUP the crop N uptake. All the components are in g N m^{-2} d^{-1}. N concentration in the soil solution (NCON, g N g^{-1} water) is obtained as:

$$NCON(L) = NSOL(L) / (WL(L) \times 1000) \qquad (20)$$

where the number 1000 converts WL(L) from mm to g. The amount of N available to the crop from the soil solution of a layer (SNAVL, g N m^{-2}) is then obtained as:

$$SNAVL(L) = (NCON(L) - 0.000001) \times WL(L) \times 1000 \times RLYER(L)/DLYER(L) \qquad (21)$$

Eq. 21 assumes no N is taken up by plants when NCON is less than 0.000001 g N g^{-1} water (1 mg N L^{-1}) and the fraction of N available to the crop from a given layer is equal to the fraction of the layer occupied by roots.

The method ignores N addition to the soil due to atmospheric reduction of N_2 as a result of lightning activity and biological fixation by free-living organisms and N removal by runoff. Mineralization of organic N to ammonium (NH_4^+) and the subsequent transformation to nitrate (NO_3^-) is modeled as one transformation, i.e. NMIN. NMIN is obtained as a function of soil potentially mineralizable N, soil soluble N and soil water and

temperature. Soil temperature is assumed equal to the air temperature. The soil N submodel allows up to 10 fertilization applications. Amount of net N in each application (NFERT) needs to be defined as N, not in the form of NO_3^- or NH_4^+. Following any fertilizer application, NVOL is calculated as a single pulse as a fraction of applied N. The fraction of N volatilized in the soil immediately following application needs to be inputted into the model for each N fertilization event. Some guidelines are provided in the model for estimating this fraction from environmental conditions, fertilizer type and application method (Delgado et al., 2010). NFERT and NVOL are considered for the first layer. NOUT is obtained as a function of soil soluble N, the amount of drained water from that layer (FLOUT) and total soil water in that layer. NOUT form user-specified layer is considered as N leaching. It is assumed that denitrification occurs whenever the water content of the first two layers exceeds the drained upper limit, i.e. FTSW>1. When FTSW>1, N loss through denitrification is obtained from soil N concentration, soil water content and temperature. NUP from each soil layer depends on the fraction of the layer explored by roots and the ratio of SNAVL in that layer to total SNAVL in the root zone.

The soil N submodel requires a measureable soil inputs: initial soil soluble N and initial soil organic N available for mineralization, as well as the time, amount and volatilization fraction of each N application. The initial soil soluble N and initial soil organic N available for mineralization are calculated from soil coarse fraction, soil bulk density, soil organic N, fraction soil organic N available to mineralization, NO_3^- content in soil solution and NH_4^+ content in soil solution (Table 2).

Model simulations

The code for the model is written in Visual Basic for Application in Excel that uses Excel's sheets for input and output. The model, including its code, can be downloaded from https://sites.google.com/site/cropmodeling. The model needs daily weather data, i.e. maximum and minimum temperatures, rainfall and solar radiation. It can be run for multiple scenarios/treatments over many years. The model reads crop management inputs from a "Management box" (Figure 5). The model operates on daily time steps. Daily and seasonal output results are generated within the model and selected data from the simulations is placed in an Excel sheet.

Table 2. A sample soil profile and soil inputs needed by the model. NLYER is the number of layers in the soil profile, LDRAIN the layer from which leaching is calculated, SALB the soil albedo, CN_2 the soil curve number, DLAYER the thickness of the layer, SAT the volumetric soil water content at saturation, DUL the drained upper limit, EXTR the extractable soil water content, DRAINF the drainage factor, MAI the soil moisture availability index, FG the coarse fraction, BDL the bulk density, NORG the organic N, FMIN the fraction of organic N that is available for mineralization, NO3 the NO_3^- concentration and NH4 the NH_4^+ concentration.

Code	Description											
EBI0001	E. Zeinali xxxx xxxx											
NLYER	LDRAIN	SALB		CN_2								
5	5	0.13		79								
		cm.cm⁻¹	cm.cm⁻¹	cm.cm⁻¹	-	-	-	g.cm⁻³	%	-	ppm mg.kg⁻¹	ppm mg.kg⁻¹
Layer#	DLYER	SAT	DUL	EXTR	DRAINF	MAI	FG	BDL	NORG	FMIN	NO_3	NH_4
1	150	0.472	0.264	0.13	0.5	0.8	0	1.4	0.1	0.1	22	2.2
2	150	0.478	0.273	0.13	0.5	0.9	0	1.38	0.1	0.1	18	1.8
3	300	0.504	0.328	0.13	0.5	0.9	0	1.31	0.06	0.1	10	1.6
4	300	0.52	0.364	0.13	0.5	0.9	0	1.27	0.04	0.05	7	1.3
5	300	0.523	0.373	0.13	0.5	0.9	0	1.26	0.02	0.05	5	1.1

Code		Description:				
Rfd-LI						
yno	FixFind	Fyear	Pdoy	PDEN		
21	1	1990	339	300		
nitrogen =	2			water =	2	IRGLVL
Number of appl. =	2			Number of irrig. =	0	0.5
DAP- or CBD-based:	2			DAP-, CBD- or DOY-based:	0	
	DAP/CBD	Amount	Frac. Vol.	DAP/CBD/DOY	Amount	
No	(-)	(g/m2)	(%)	(-)	(mm)	
1	1	2.3	2			
2	10	3.45	10			
3						
4						
5						
6						
7						
8						
9						
10						

Figure 5. Appearance of a "Management Box" that includes controls for sowing, irrigation and nitrogen management.

Model testing

The capability of the model to simulate crop yield under a wide range of growth and environmental conditions was evaluated using independent data sets from Gorgan region, Iran (Table 1). To simulate these crops the relevant input requirements were collected. Actual maximum and minimum temperatures, rainfall and solar radiation (derived from sunshine hours) were available for each experiment. Date of sowing and plant density were inputted from known values for each experiment and soil water and nitrogen attributes were derived from measurements or from the known values for similar soil types. All parameters related to the cultivars are given in Appendix I as estimated by Soltani and Maddah (2013) from a separate data set (Table 1).

Results and Discussion

Studies listed in Table 1 reported wheat development, growth and yield under a wide range of sowing dates and densities and nitrogen rates in Gorgan, Iran. Maddah (2007) compared growth and yield of two wheat cultivars and two chickpea cultivars under optimal conditions. Jafari (2008) studied response of growth and yield to plant density (50-500 plant m^{-2}) in two cultivars. Zeinali (2009) evaluated crop growth and yield of wheat crops in 17 farmers' fields. Dasmalchi (2010) studied response of

development, growth and yield of three wheat cultivars to a very wide range of sowing dates. Hoseeini (2010) evaluated response of three cultivars to nitrogen fertilizer from 0 to 122 kg N ha^{-1}. Zahed (2010) evaluated growth and yield in response to plant density in some cultivars. Jafari (2009) and Dastmalchi (2010) included sowing density and date, respectively, that are not necessarily representative of common practices by farmer, but they offered results from a wide range of environmental and growth conditions.

A sample simulated and measured dynamics of crop LAI, total and seed dry matter and total N accumulation is presented in Figure 6. The measured data belonged to a wheat crop sown on 16 December 2005 at a density of 333 plants per m^{-2} in Gorgan, Iran. Overall, the model successfully simulated these attributes, although there are some discrepancies between measured and simulated data.
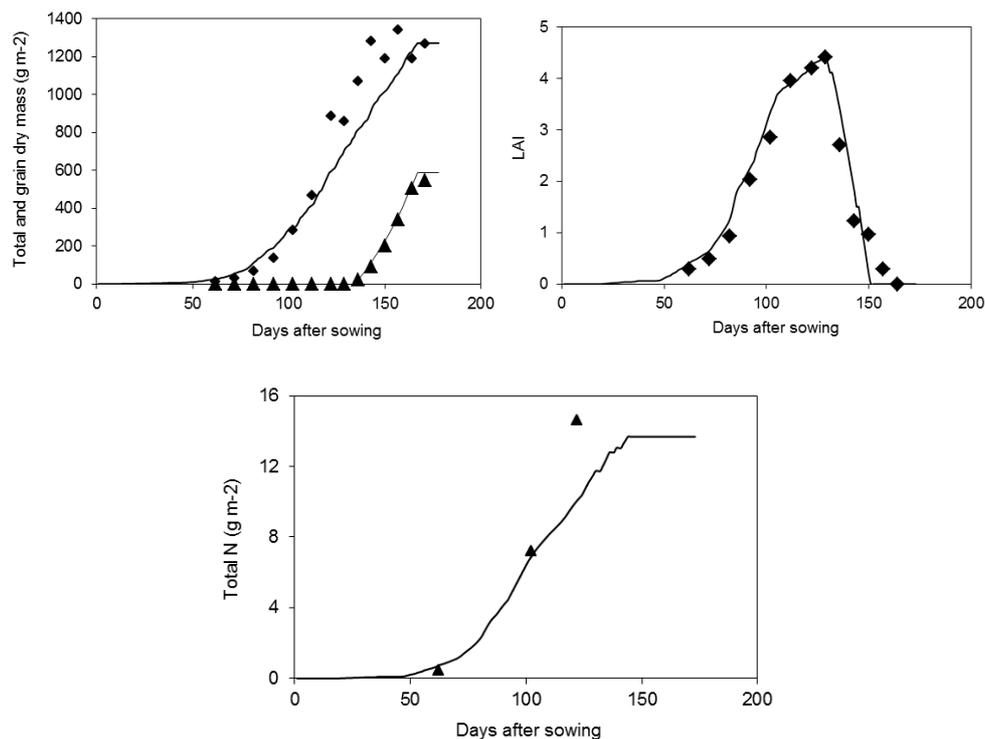
Figure 6. Simulated and measured values of leaf area index (LAI), total and seed dry matter and total N accumulation by a wheat crop sown on 16 December 2005 at density of 333 plants per m^{-2} at Gorgan, Iran (Maddah, 2007).

Days to anthesis observed over all experiments ranged between 47 and 127 d with an average of 107 d (Figure 7). The observed range in days to maturity was between 82 and 175 d with an average of 147d. The model simulated both anthesis date and maturity date with a coefficient of variation (CV) of less than 6% and a correlation coefficient of higher than 0.95 (Figure 7).
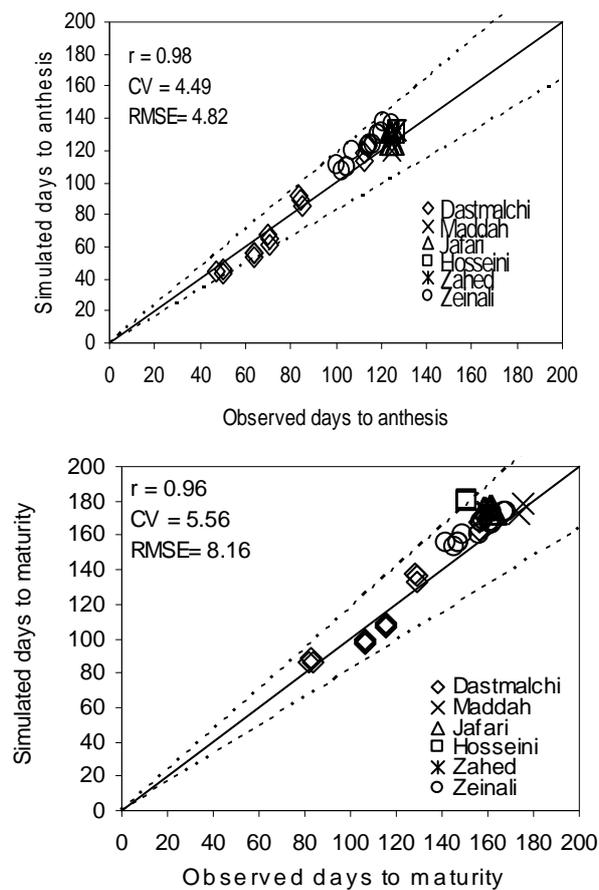

Figure 7. Simulated versus measured days to anthesis and maturity. The 20% ranges of discrepancy between simulated and measured are indicated by dashed lines. Solid line is 1:1 line.

The model performance across experiments was not as accurate as phenological stages for LAI at anthesis and crop cumulative mass at

anthesis and maturity. RMSE of model prediction for LAI at anthesis was 0.48 m^2 m^{-2} which was 11.8% of observed mean (CV=11.8%). The correlation coefficient between observed and simulated LAI was 0.8 (Figure 8). The model showed a similar performance for crop dry matter at anthesis and maturity. CV for these two was less than 10% and correlation coefficient was higher than 0.7. RMSE was 62 g m^{-2} for crop mass at anthesis and 90 g m^{-2} for crop mass at maturity (Figure 9). It was concluded the model was robust in simulating LAI and crop mass considering the wide and unusual range of sowing times and densities and nitrogen fertilizer used in the experiments and the difficulty of measuring leaf area and dry mass under field conditions (i.e. the common existence of a higher CV for observed data).

Figure 10 indicates model performance for crop grain yield. Observed grain yield varied between 94 and 591 g m^{-2} with a mean of 427g m^{-2}. In most cases, simulated grain yield was similar to observed yields with a RMSE of 38 g m^{-2} which was 8% of average measured yield. The majority of the data points are scattered around 1:1 line and occurred between 18% discrepancy lines. The correlation coefficient between simulated and measured yields was 0.89.
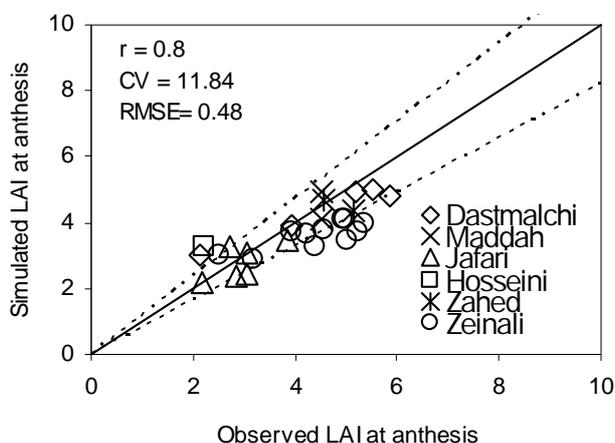

Figure 8. Simulated versus measured LAI at anthesis. The 20% ranges of discrepancy between simulated and measured are indicated by dashed lines. Solid line is 1:1 line.
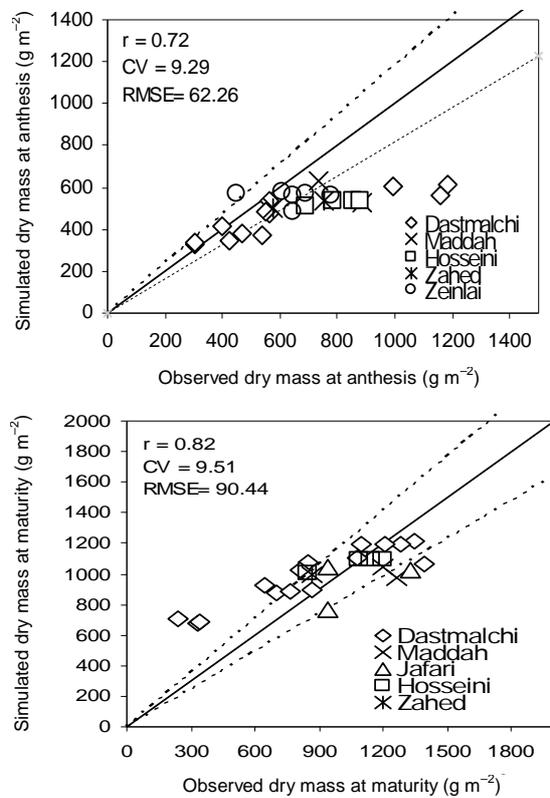
Figure 9. Simulated versus measured crop mass at anthesis and maturity. The 20% ranges of discrepancy between simulated and measured are indicated by dashed lines. Solid line is 1:1 line.
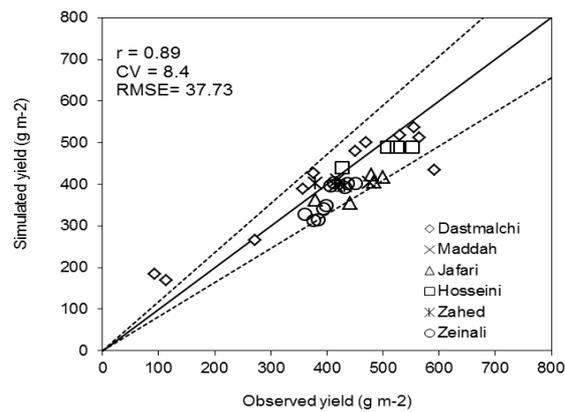

Figure 10. Simulated versus measured grain yield. The 20% ranges of discrepancy between simulated and measured are indicated by dashed lines. Solid line is 1:1 line.

Form the general agreement between simulated and observed values of days to anthesis and maturity, crop LAI and dry mass at anthesis and crop total mass and grain yield at maturity under a diverse range of growth and environmental conditions for different cultivars we conclude that the model has a robust predictive capability. Soltani et al. (2010) evaluated wheat models of DSSAT, CropSyst and APSIM for the same location and cultivars. The current model (SSM-Wheat) performance is similar to those models (data not shown) although the current model is comparatively simple. Comparison of the mentioned wheat models is the subject of another paper from the same authors which is under preparation.

Simulating crop phenology and dry matter production in SSM-wheat is similar to that of DSSAT and APSIM wheat models. However, SSM-wheat simulates dry matter distribution and LAI development and senescence using new, different algorithms which require fewer parameters. Plant N balance is simulated using an approach (Sinclair et al., 2003) that is more physiologically-based and requires much less parameters. Yield formation method is also different and is based on a new, modified linear increase in harvest index approach (Soltani and Sinclair, 2011). SSM-wheat also uses much simpler soil water- and N-balance subroutines that require less input information and parameters. The major advantages of SSM-wheat are, in our opinion, its transparency and ease-to-use.

Overall, it can be concluded that the model can be used for the objectives such as analysis of crop yield and its limitations in response to environmental conditions, management inputs and genetic factors.

Acknowledgment

References

Ahmadi, M., 2008. Predicting phonological development in wheat (*Triticum aestivum* L.). Dissertation for M.Sc. degree in Agronomy. Department of Agronomy, Gorgan University of Agricultural Science and Natural Resources. 93p. (text in Persian with English abstract)

Amir, J., Sinclair, T.R., 1991. A model of water limitation on spring wheat growth and yield. Field Crops Res. 29, 59-69.

Arabameri, R., 2008. Predicting kernel number and biomass retranslocation in wheat (*Triticum aestivum* L.). Dissertation for M.Sc. degree in Agronomy. Department of Agronomy, Gorgan University of Agricultural Science and Natural Resources. 90p. (text in Persian with English abstract)

Arabameri, R., Soltani, A., Kamkar, B., Zainali, E., Khavari, F., 2010. Determination parameters simulation yield by harvest index in wheat. J. Plant Prod. 17 (2), 137-150. (text in Persian with English abstract)

Bakhshandeh, E., 2011. Evaluation of allometric relationships in wheat cultivars of Golestan province. Dissertation for M.Sc. degree in Agronomy. Department of Agronomy, Gorgan University of Agricultural Science and Natural Resources. 118p. (text in Persian with English abstract)

Dardanelli, D.L., Ritchie, J.T., Calmon, M., Andriani, J.M., Collino, D.J., 2004. An empirical model for root water uptake. Field Crops Res. 87, 59-71.

Dastmalchi, A., 2010. Simulating wheat growth and development using CropSyst model under Gorgan conditions. Dissertation for M.Sc. degree in Agronomy. Department of Agronomy, Gorgan University of Agricultural Science and Natural Resources. 105p. (text in Persian with English abstract)

Delgado, J.A., Gagliardi, P., Shaffer, M.J., Cover, H., Hesketh, E., 2010. New tools to assess nitrogen management for conservation of our biosphere. In: J.A. Delgado and R.F. Follett (Editors.) Advances in Nitrogen Management for Water Quality. SWCS, Ankeny IA, USA. pp. 373-409.

Fletcher, A.L., Jamieson, P.D., 2006. Causes of variation in the rate of increase of wheat harvest index. Field Crops Res. 113, 268-273.

Ghadiryan, R., 2011. Growth analysis of wheat cultivars of Golestan province. Dissertation for M.Sc degree in Agronomy. Azad University of bojnord. 117p. (text in Persian with English abstract)

Hosseini, R., 2010. The effect of nitrogen on nitrogen use efficiency and radiation use efficieny in modern and old wheat cultivars. Dissertation for M.Sc degree in Agronomy. Department of Agronomy, Gorgan University of Agricultural Science and Natural Resources. (text in Persian with English abstract)

Jafari, M., 2008. Modeling of density effect on leaf appearance and senescence in wheat. Dissertation for M.Sc. degree in Agronomy. Department of Agronomy, Gorgan University of Agricultural Science and Natural Resources. 94p. (text in Persian with English abstract)

Jones, J.W., Hoogenboom, G., Porter, C.H., Boote, K.J., Batchelor, W.D., Hunt, L.A., Wilkens, P.W., Singh, U., Gijsman, A.J., Ritchie, J.T., 2003. The DSSAT cropping system model. Eur. J. Agron. 18, 235-265.

Khavari, F., 2008. Modeling leaf appearance and senescence in wheat cultivars. Dissertation for M.Sc. degree in Agronomy. Azad University of bojnord. 93p. (text in Persian with English abstract)

Maddah, V., 2007. Comparative physiology ofwheat and chickpea.MS thesis, Faculty of Agriculture, Gorgan University of Agricultural Sciences and Natural Resources, Gorgan, Iran. (text in Persian with English abstract).

Mc Master, G.S., White, J.W., Weiss, A., Baenziger, P.S., Wilhelm, W.W., Porter, J.W., Jamieson, P.D., 2009. Simulating crop phenological responses to water deficits. In: Ahuja, L.R., Reddy, V.R., Anapalli, S.A. and Yu, Q. (Editors), Modeling the Response of Crops to Limited Water: Recent Advances in Understanding and Modeling Water Stress Effects on Plant Growth Processes. Vol. 1 of series: Advances in Agricultural Systems Modeling. Transdisciplinary Research, Synthesis and Applications. ASA-SSA-CSSA, Madison, WI, USA. pp. 277-300.

Mirdavardoost, F., 2008. Quantifying of vernalization response in some Iranian wheat. Dissertation for M.Sc. degree in Agronomy. Department of Agronomy, Gorgan University of Agricultural Science and Natural Resources. 87p. (text in Persian with English abstract)

Priestley, C.H.B., Taylor, R.J., 1972. On the assessment of surface heat flux and evaporation using large-scale parameters. Mon. Weather Rev. 100, 81-92.

Ritchie, J.T., 1991. Wheat phasic development. In: Hanks, R.J., Ritchie, J.T. (Editors), Modeling Plant and Soil Systems. Agronomy Monograph, 31, 31-54.

Ritchie, J.T., 1998. Soil water balance and plant water stress. In: Tsuji, G.Y., Hoogenboom, G., Thornton, P.K. (Editors), Understanding Options for Agricultural Production. Kluwer Academic Publishers, Dordretcht, pp. 41-54.

Sinclair, T.R., 1994. Limits to crop yield? In: Boote, K.J., Bennett, J.M., Sinclair, T.R. and Paulsen, G.M. (Editors), Physiology and Determinations of Crop Yield, Am. Soc. Agron., Madison, WI. pp. 509-532.

Sinclair, T.R., Amir, J., 1992. A model to assess nitrogen limitations on the growth and yield of spring wheat. Field Crops Res. 30, 1-11.

Sinclair, T.R., Farias, J.R., Neumaier, N., Nepomuceno, A.L., 2003. Modeling nitrogen accumulation and use by soybean. Field Crops Res. 81, 149-158.

Sinclair, T.R., Messina, C.D., Beatty, A., Samples, M., 2010. Assessment across the United States of the benefits of altered soybean drought traits. Agron. J. 102, 475-482.

Sinclair, T.R., Muchow, R.C., 1995. Effect of nitrogen supply on maize yield: I. Modeling physiological responses. Agron. J. 87, 632-641.

Sinclair, T.R., Muchow, R.C., Monteith, J.L., 1997. Model analysis of sorghum response to nitrogen in subtropical and tropical environments. Agron. J. 89, 201-207.

Soltani, A., Mahru-Kashani, A.H., Dastmalchi, A., Maddah, V., Zeinali, E., Kamkar, B., 2010. Simulating wheat development and growth by DSSAT, CropSyst and APSIM models under Gorgan and Gonbad environmental conditions. GUSNR, Research Report.

Soltani, A., Hammer, G.L., Torabi, B., Robertson, M.J., Zeinali, E., 2006a. Modeling chickpea growth and development: phenological development. Field Crops Res. 99, 1-13.

Soltani, A., Robertson, M.J., Mohammad-Nejad, Y., Rahemi-Karizaki, A., 2006b. Modeling chickpea growth and development: leaf production and senescence. Field Crops Res. 99, 14-23.

Soltani, A., Robertson, M.J., Rahemi-Karizaki, A., Poorreza, J., Zarei, H., 2006c. Modeling biomass accumulation and partitioning in chickpea (*Cicer arietinum* L.). J. Agron. Crop Sci. 192, 379-389.

Soltani, A., Hoogenboom, G., 2007. Assessing crop management options with crop simulation models based on generated whether data. Field Crops Res. 103, 198-207.

Soltani, A., Sinclair, T.R., 2011. A simple model for chickpea development, growth and yield. Field Crops Research. 124, 252-260.

Soltani, A., Sinclair, T.R., 2012a. Modeling Physiology of Crop Development, Growth and Yield. CABI publication. 322p.

Soltani, A., Sinclair, T.R., 2012b. Optimizing chickpea phenology to available water under current and future climates. Eur. J. Agron. 38, 22-31.

Soltani, A., Sinclair, T.R., 2012c. Identifying plant traits to increase chickpea yield in water-limited environments. Field Crops Research. 133, 186-196.

Soltani, A., Khooie, F.R., Ghassemi-Golezani, K., Moghaddam, M., 2001a. A simulation study of chickpea crop response to limited irrigation in a semiarid environment. Agric. Water Manag. 49, 225-237.

Soltani, A., Maddah, V., 2013. Parameterization and evaluation of SSM-Wheat model for Gloestan province cultivars. GUASNR, Research Report.

Soltani, A., Zeinali, E., Galeshi, S., 2001b. Simulating Geophysical Fluid Dynamics Laboratory predicted climate change impacts on rice cropping in Iran. J. Agric. Sci. Technol. (Tehran) 3, 81-90.

Tanner, C.B., Sinclair, T.R., 1983. Efficient water use in crop production: Research or research? In: Taylor, H.M., Jordan, W.R., Sinclair, T.R. (Editors.), Limitations to efficient water use in crop production. ASA, CSSA and SSSA, Madison, WI. pp. 1-27.

Van Laar, H.H., Goudriaan, J., Van Keulen, H., 1997. SUCROS97: Simulation of crop growth for potential and water-limited production situations. Quantitative Approaches in Systems Analysis No., September 1997. AB-DLO, Wageningen, the Netherlands.

Williams, J.R., Jones, C.A., Kiniry, J.A., Spanel, D.A., 1989. The EPIC crop growth model. Trans. ASAE. 32, 497-510.

Zafari, A., 2013. Allometric relationships in wheat as influenced by plant density. Dissertation for M.Sc. degree in Agronomy. Department of Agronomy, Gorgan University of Agricultural Science and Natural Resources. (text in Persian with English abstract; under preparation)

Zahed, M., 2010. The effect of plant density on nitrogen use efficiency and radiation use efficieny in modern and old wheat cultivars. Dissertation for M.Sc. degree in Agronomy. Department of Agronomy, Gorgan University of Agricultural Science and Natural Resources. (text in Persian with English abstract)

Zeinali, E., 2009. Wheat Nitrogen Nutrition in Gorgan; Agronomical Physiological and Enviromental Aspects. A Thesis Submitted for the Degree of Ph.D. in Agronomy, Gorgan University of Agricultural Science and Natural Resources. 201p. (text in Persian with English abstract)

Appendix I. List of model parameters and their estimates for Golestan province cultivars according to Soltani and Maddah (2013).

Parameter	Abbreviation	Unit	Zagros	Tajan	Koohdasht	Shirudi
Base temperature for development	TBD	^{o}C	0	0	0	0
Optimal temperature for development	TP1D	^{o}C	27.5	27.5	27.5	27.5
Ceiling temperature for development	TCD	^{o}C	40	40	40	40
Base temperature for vernalization	TBVER	^{o}C	-1	-1	-1	-1
Lower optimal temp for vernalization	TP1VER	^{o}C	0	0	0	0
Upper optimal temp for vernalization	TP2VER	^{o}C	8	8	8	8
Ceiling temperature for vernalization	TCVER	^{o}C	12	12	12	12
Vernalization saturation days	VDSAT	d	50	50	50	50
Vernalization sensitivity coefficient	vsen	-	0.00305	0.00089	0	0.00089
Critical photoperiod	cpp	^{o}C	21	21	21	21
Photoperiod sensitivity coefficient	ppsen	^{o}C	0.001649	0.001467	0.00531	0.00263
Biological day (bd) from sowing to emergence	bdSOWEMR	d	4	4	4	4
bd from emergence to first-tiller	bdEMRTIL	d	5.5	5.5	5.5	4.5
bd from first-tiller to first node	bdTILSEL	d	8.04	12.67	8.71	10.05
bd from first-node to booting	bdSELBOT	d	7	6	6	8
bd from booting to ear emergence	bdBOTEAR	d	2	2	2	3
bd from ear emergence to anthesis	bdEARANT	d	7	8	9	7
bd from anthesis to physiological maturity	bdANTPM	d	34	34	33	34
bd from physiological to harvest maturity	bdPMHM	d	8	8	8	8
Phyllochron	phyl	^{o}C / leaf	91	95	100	112
Constant in power eq ($y=ax^b$) for plant leaf area versus main stem leaf number	PLACON	-	1	1	1	1
Exponent in power eq ($y=ax^b$) for plant leaf area versus main stem leaf number	PLAPOW300	-	2.34	2.34	2.34	2.34
Specific leaf area	SLA	m^2 /g	0.021	0.021	0.021	0.021
Critical minimum temp for leaf destruction due to frosts	TKILL	^{o}C	-5	-5	-5	-5
Fraction leaf destruction below the critical by each degree centigrad	FRZLDR	$m^2/m^2/^oC$	0.1	0.1	0.1	0.1
Base temperature for RUE	TBRUE	^{o}C	0	0	0	0
Lower optimal temp for RUE	TP1RUE	^{o}C	15	15	15	15
Upper optimal temp for RUE	TP2RUE	^{o}C	22	22	22	22

Continue Appendix I.

Parameter	Abbreviation	Unit	Zagros	Tajan	Koohdasht	Shirudi
Ceiling temperature for RUE	TCRUE	^{o}C	35	35	35	35
Extinction coefficient	KPAR	-	0.65	0.65	0.65	0.65
Potential RUE	IRUE	g / MJ	2.2	2.2	2.2	2.2
A partitioning coefficient to leaves	FLF1A	g/g	0.6	0.6	0.6	0.6
A partitioning coefficient to leaves	FLFL1B	g/g	0.3	0.3	0.3	0.3
Critical crop mass for FLF1A to FLF1B	WTOPL	g / m^2	160	160	160	160
A partitioning coefficient to leaves	FLF2	g / g	0.1	0.1	0.1	0.1
Fraction translocation to grains	FRTRL	-	0.22	0.22	0.22	0.22
Grain conversion coefficient	GCC	-	1	1	1	1
Potential slope of harvest index (DHI)	PDHI	g/g/d	0.014	0.014	0.014	0.014
A critical point for DHI	WDHI1	g/m^2	0	0	0	0
A critical point for DHI	WDHI2	g/m^2	600	600	600	600
A critical point for DHI	WDHI3	g/m^2	1200	1200	1200	1200
A critical point for DHI	WDHI4	g/m^2	3200	3200	3200	3200
Depth of roots at emergence	IDEPORT	mm	200	200	200	200
Maximum effective extraction depth	MEED	mm	1000	1000	1000	1000
Potential root growth	GRTDP	mm/bd	30	30	30	30
Transpiration efficiency coefficient	TEC	Pa	5.8	5.8	5.8	5.8
FTSW threshold for growth	WSSG	-	0.3	0.3	0.3	0.3
FTSW threshold for leaf expansion	WSSL	-	0.4	0.4	0.4	0.4
FTSW threshold for development	WSSD	-	0.5	0.5	0.5	0.5
Killing no. of consecutive flooding	FLDKL	d	20	20	20	20
Specific leaf N, green leaves	SLNG	g m^{-2}	1.5	1.5	1.5	1.5
Specific leaf N, senesced leaves	SLNS	g m^{-2}	0.4	0.4	0.4	0.4
Stem N content, green stems	SNCG	g g^{-1}	0.015	0.015	0.015	0.015
Stem N content, senesced stems	SNCS	g g^{-1}	0.005	0.005	0.005	0.005
Grain N content	GNC	g g^{-1}	0.0213	0.0213	0.0213	0.0213
Maximum N uptake rate	MXNUP	g m^{-2}d^{-1}	0.25	0.25	0.25	0.25